doi:10.1093/brain/aww331 BRAIN 2017: 140; 721–734 | 721

BRAIN
A JOURNAL OF NEUROLOGY

Dopamine controls Parkinson's tremor by inhibiting the cerebellar thalamus

Michiel F. Dirkx,[1,2] Hanneke E. M. den Ouden,[1] Esther Aarts,[1] Monique H. M. Timmer,[1,2] Bastiaan R. Bloem,[2] Ivan Toni[1] and Rick C. Helmich[1,2]

Parkinson's resting tremor is related to altered cerebral activity in the basal ganglia and the cerebello-thalamo-cortical circuit. Although Parkinson's disease is characterized by dopamine depletion in the basal ganglia, the dopaminergic basis of resting tremor remains unclear: dopaminergic medication reduces tremor in some patients, but many patients have a dopamine-resistant tremor. Using pharmacological functional magnetic resonance imaging, we test how a dopaminergic intervention influences the cerebral circuit involved in Parkinson's tremor. From a sample of 40 patients with Parkinson's disease, we selected 15 patients with a clearly tremor-dominant phenotype. We compared tremor-related activity and effective connectivity (using combined electromyography-functional magnetic resonance imaging) on two occasions: ON and OFF dopaminergic medication. Building on a recently developed cerebral model of Parkinson's tremor, we tested the effect of dopamine on cerebral activity associated with the onset of tremor episodes (in the basal ganglia) and with tremor amplitude (in the cerebello-thalamo-cortical circuit). Dopaminergic medication reduced clinical resting tremor scores (mean 28%, range −12 to 68%). Furthermore, dopaminergic medication reduced tremor onset-related activity in the globus pallidus and tremor amplitude-related activity in the thalamic ventral intermediate nucleus. Network analyses using dynamic causal modelling showed that dopamine directly increased self-inhibition of the ventral intermediate nucleus, rather than indirectly influencing the cerebello-thalamo-cortical circuit through the basal ganglia. Crucially, the magnitude of thalamic self-inhibition predicted the clinical dopamine response of tremor. Dopamine reduces resting tremor by potentiating inhibitory mechanisms in a cerebellar nucleus of the thalamus (ventral intermediate nucleus). This suggests that altered dopaminergic projections to the cerebello-thalamo-cortical circuit have a role in Parkinson's tremor.

1 Donders Institute for Brain, Cognition and Behavior, Radboud University, 6500 HB Nijmegen, The Netherlands
2 Radboud University Medical Centre, Donders Institute for Brain, Cognition and Behaviour, Department of Neurology and Parkinson Centre Nijmegen (ParC), 6500 HB Nijmegen, The Netherlands

Correspondence to: Michiel F. Dirkx,
Radboud University Medical Centre,
Neurology department (HP 935), PO Box 9101,
6500 HB Nijmegen,
The Netherlands
E-mail: michiel.dirkx@radboudumc.nl

Keywords: Parkinson's disease; resting tremor; dopamine; resting state functional MRI; dynamic causal modelling

Abbreviations: BOLD = blood oxygenation level-dependent; DCM = dynamic causal modelling; GPe/i = globus pallidus externa/interna; STN = subthalamic nucleus; UPDRS = Unified Parkinson's Disease Rating Scale; VIM = ventral intermediate nucleus of the thalamus; VLa/d/p/vp = ventrolateral thalamus anterior/dorsal/posterior/ventral posterior

Received July 29, 2016. Revised October 18, 2016. Accepted November 14, 2016. Advance Access publication January 10, 2017

Introduction

Parkinson's disease is a progressive neurodegenerative disorder characterized by bradykinesia, rigidity and a 4–6 Hz resting tremor. The pathological hallmark of Parkinson's disease is nigro-striatal dopamine depletion (Kish *et al.*, 1988). However, in contrast to bradykinesia and rigidity, the relation between tremor and dopamine (depletion) is unclear. For example, the response of tremor to dopaminergic medication varies greatly between patients, with some patients exhibiting a remarkable dopamine-resistant tremor (Pogarell *et al.*, 2002; Fishman, 2008). Furthermore, unlike other motor symptoms, tremor does not correlate with striatal dopamine depletion (Pirker, 2003). Instead, it has been suggested that resting tremor is linked to pallidal dopamine depletion (Mounayar *et al.*, 2007; Helmich *et al.*, 2011) or to abnormalities in the noradrenergic (Isaias *et al.*, 2011) and serotonergic systems (Doder *et al.*, 2003; Qamhawi *et al.*, 2015). Here we aimed to resolve these discrepancies by investigating the cerebral mechanisms underlying the effect of dopaminergic medication on resting tremor in patients with Parkinson's disease.

We previously reported that resting tremor results from an interaction between the basal ganglia and a cerebello-thalamo-cortical motor loop consisting of motor cortex, ventral intermediate part of the thalamus (VIM) and cerebellum (Helmich *et al.*, 2011). Specifically, we found that the internal globus pallidus (GPi) drives tremulous activity in a cerebello-thalamo-cortical motor loop through the motor cortex (Dirkx *et al.*, 2016). However, it remains unclear how dopamine influences this circuit, and why there are such considerable interindividual differences in the clinical response of resting tremor to dopaminergic medication. Given that the basal ganglia receive massive dopaminergic projections from the midbrain (Lindvall and Bjorklund, 1974), and that pallidal dopamine depletion is correlated with tremor severity (Helmich *et al.*, 2011), this region appears the most likely target for dopaminergic medication. However, there is evidence that the regions of the cerebello-thalamo-cortical motor loop are also sensitive to dopamine. More specifically, the presence of the dopamine transporter (DAT) in the human VIM (Sanchez-Gonzalez *et al.*, 2005; Garcia-Cabezas *et al.*, 2009) indicates that the ventrolateral thalamus receives dopaminergic projections. Furthermore, there is widespread dopaminergic innervation of the cerebral cortex in primates, with the primary motor cortex being most densely targeted (Berger *et al.*, 1991). Indeed, dopaminergic medication has been found to specifically reduce tremor-related oscillatory coupling between thalamus and motor cortex in Parkinson's disease (Pollok *et al.*, 2009). Finally, dopaminergic receptors are also present in the cerebellum, albeit more sparsely (Hurley *et al.*, 2003).

Here, we investigate the effects of dopamine on tremor-related activity in a cerebral network consisting of basal ganglia (internal and external globus pallidus, subthalamic nucleus) and a cerebello-thalamo-cortical motor loop in patients with Parkinson's disease (Helmich *et al.*, 2012; Dirkx *et al.*, 2016). Specifically, we investigated the effects of dopamine on tremor-related cerebral activity and effective connectivity (i.e. the influence that neural nodes exert over another) within the tremor network, and related these effects to individual clinical tremor improvements. Furthermore, we distinguished between cerebral activity related to fluctuations in tremor amplitude and changes in tremor amplitude (Helmich *et al.*, 2011). To this end, we used concurrent functional MRI and EMG recordings acquired during resting tremor episodes of Parkinson's disease patients both OFF and ON dopaminergic medication.

Materials and methods

Subjects and inclusion

We sampled patients from a larger database consisting of 40 patients with Parkinson's disease that were tested ON and OFF dopaminergic medication in two functional MRI sessions. For this study, we only included Parkinson's disease patients with resting tremor during functional MRI scanning in both sessions. This is important, because our method requires the presence of tremor (assessed using EMG) to identify and characterize tremor-related cerebral activity and connectivity (assessed using functional MRI). Therefore, we included idiopathic Parkinson's disease patients with: (i) a clinical resting tremor [defined as Unified Parkinson's Disease Rating Scale (UPDRS) resting tremor score for one arm of $\geqslant 1$ point and a history of tremor]; and (ii) resting tremor during both functional MRI sessions (defined as a 4–6 Hz peak in the EMG power spectrum and presence of tremor bursts in the EMG). This led to the inclusion of 15 patients [seven male; aged 56 ± 2 years; average $\pm$ standard error of the mean (SEM)]. None of these patients had cognitive dysfunction [Mini-Mental State Examination (MMSE) <24], neurological/psychiatric comorbidity, severe head-tremor or severe dyskinesias. Additional disease characteristics are specified in Table 1. Clinical dopamine response was defined as the absolute difference between UPDRS scores OFF and ON dopaminergic medication.

Image acquisition and preprocessing

Functional MRI was performed on a 3 T MRI system (Siemens) in two sessions on separate days. The order of sessions was pseudorandomized between patients. Patients were asked to take their normal dopaminergic medication at 8:30 am on one occasion ('ON'; levodopa equivalent daily dosage = 389 ± 63 mg, mean ± SEM), and to abstain from this medication ('relative OFF') for at least 18 h prior to testing on the other occasion (48 h for ropinirole prolonged release tablets). The average time of intake of dopaminergic medication to start of scanning was 2 h 4 min ± 8 min [mean ± standard deviation (SD)]. Subjects were instructed to lie still with eyes open, which we confirmed with online eye-tracking. We used a multi-echo echo planar imaging sequence (echo time 1 = 9.4 ms; echo time 2 = 21.2 ms; echo time 3 = 33 ms/echo

Table 1 Clinical characteristics of subjects

Characteristic	Mean (+SD)		
Disease duration (years)	4.2 (2.2)		
Hoehn and Yahr	2 (1–3)		
FAB	17.1 (0.9)		
UPDRS	**OFF**	**ON**	***P***
Total	27.9 (6.1)	20.7 (4.5)	<0.001
Non-tremor (B + R)			
Most	9.7 (3.4)	7.5 (2.8)	0.001
Least	4.0 (1.8)	2.5 (2.2)	0.002
Axial	6.1 (2.4)	4.4 (1.4)	0.001
Rest tremor			
Most	3.2 (1.5)	2.3 (1.3)	0.01
Least	0.9 (1.6)	0.3 (0.9)	0.03
Patient ID	**Medication**		
P01	Levodopa/carbidopa 250 mg/day, pramipexole 0.357 mg/day		
P02	Ropinorole 8 mg/day		
P03	Ropinorole 8 mg/day		
P04	Levodopa/benserazide 550 mg/day, ropinorole 12 mg/day		
P05	Levodopa/carbidopa 300 mg/day		
P06	Levodopa/carbidopa 125 mg/day, pramipexole 3.15 mg/day		
P07	Pramipexole 4.5 mg/day		
P08	Levodopa/carbidopa 125 mg/day, ropinorole 8 mg/day		
P09	Levodopa/carbidopa 250 mg/day		
P10	Levodopa/benserazide 250 mg/day		
P11	Ropinorole 12 mg/day, amantadine 200 mg/day		
P12	Levodopa/benserazide 1000 mg/day, ropinorole 4 mg/day		
P13	Levodopa/carbidopa 650 mg/day		
P14	Levodopa/benserazide 150 mg/day		
P15	Levodopa/benserazide 250 mg/day, pramipexole 1.5 mg/day		

Disease characteristics of all patients are shown (Hoehn and Yahr: median, minimum and maximum scores in parentheses; other parameters: mean, standard deviation in parentheses). Disease severity of each patient was measured using the Hoehn and Yahr stages (maximum is 5) stages and the UPDRS (maximum score is 108). UPDRS scores are compared between sessions (two-sample *t*-test, two-tailed). B + R = limb bradykinesia and rigidity (sum of UPDRS items 22–26). Axial referrers to axial symptoms (sum of UPDRS items 18, 19, 22, and 27–31). Rest tremor refers to UPDRS item 20. The Frontal Assessment Battery (FAB) was used as a measure of cognitive function (maximum is 18). Duration was defined as the time since subjective symptom onset (in years).

time 4 = 45 ms; repetition time = 1820 ms; 35 axial slices; voxel size = 3.5 × 3.5 × 3.0 mm; interslice gap = 0.5 mm; field of view = 224 mm; scanning time = ~8 min; 300 images). Additionally, a high-resolution T_1-weighted anatomical image was obtained. The first 30 volumes collected were used to estimate weights for a blood oxygenation level-dependent (BOLD) contrast-to-noise ratio map (CNR map) for each echo. Weighted summation was then used to combine all four echoes.

Functional MRI first-level analyses were done using SPM12 (Wellcome Trust Centre for Neuroimaging, London, UK; http://www.fil.ion.ucl.ac.uk). All functional images were first (i) realigned; (ii) slice time corrected to the first slice; (iii) coregistered to a structural MRI image; (iv) normalized to MNI space using unified segmentation; and (v) spatially smoothed using an 8 mm Gaussian kernel. We used several analyses to verify that head movements did not differ between sessions (Supplementary Table 1).

Tremor-related EMG activity

Muscle activity of the most-affected forearm (wrist flexors and extensors) was measured using magnetic resonance-compatible EMG (Brain Products; sampling frequency = 5000 Hz) during scanning in all 15 patients. We used Brainvision Analyzer 2.0 (Brain Products, Germany) for preprocessing and FieldTrip (Oostenveld *et al.*, 2011) for time-frequency analyses. We performed the same analysis as described in our previous study (Helmich *et al.*, 2011). Preprocessing included (i) magnetic resonance artefact correction; (ii) downsampling to 1000 Hz; (iii) filtering with a 20–200 Hz bandpass filter to remove movement artefacts; and (iv) rectifying the signal to enhance the information on EMG burst-frequency (tremor) of the signal. Subsequently, we calculated the time–frequency representations between 1–20 Hz in steps of 0.1 s using a 2-s Hanning taper, resulting in a 0.5 Hz resolution. By averaging over all time points we obtained an average power spectrum across segments. For each patient, we calculated the time course of EMG power at each subject's individual tremor frequency. The average tremor frequency across subjects was not significantly different between sessions (OFF: 4.6 ± 0.2 Hz; ON: 4.5 ± 0.1 Hz; mean ± SEM). This resulted in patient-specific regressors describing fluctuations in tremor amplitude (EMG-amp). To remove outliers, we calculated the logarithmic values of the EMG-amp and z-normalized the data within subjects. To capture activity related to changes in tremor amplitude, we calculated the first temporal derivative of the EMG-amp regressor (EMG-change). Importantly, there were no

significant differences in EMG variance [as determined by the coefficient of variation (COV)] between both sessions [EMG-amp, OFF COV = 67.1, ON COV = 35.1 ($P = 0.77$; two-tailed t-test); EMG-change, OFF COV = −32.2, ON COV = −45.8 ($P = 0.92$; two-tailed t-test)].

Tremor-related brain activity

After convolution of both EMG regressors with a haemodynamic response function, we considered EMG-amp and EMG-change as explanatory variables in a multiple regression analysis. The first-level general linear model (GLM) also included separate regressors of no interest: average signal across the whole brain (global signal to correct for head motion; Power *et al.*, 2014), in the bilateral ventricles, and over a blank portion of the magnetic resonance images (Out-of-Brain signal). Furthermore, we included 36 regressors describing head motion based on linear, quadratic and cubic effects of the six movement parameters belonging to each volume as well as the first and second derivative of each of those regressors (to control for spin-history effects) (Lund *et al.*, 2005). Each GLM contained both sessions. Parameter estimates for all regressors were then obtained by maximum likelihood estimation.

First level contrast images were entered into second-level one sample t-tests (random effects analysis) to test for group effects for the following contrasts: tremor-related activity (EMG-amp and EMG-change per session and averaged over sessions) as well as dopaminergic effects on tremor-related activity (EMG-amp and EMG-change in OFF > ON).

Regions of interest

We tested for tremor-related cerebral activity in predefined regions based on a previously defined tremor network in Parkinson's disease (Dirkx *et al.*, 2016). Specifically, we looked for (effects of dopamine on) tremor amplitude-related activity in the cerebello-thalamo-cortical motor circuit, i.e. the motor cortex [Brodmann area (BA)4/BA6, 3712 mm^3], VIM (968 mm^3) and cerebellum (Lobule V/VI; 1416 mm^3) (Timmermann *et al.*, 2003; Helmich *et al.*, 2011). Furthermore, we looked for (effects of dopamine on) activity related to changes in tremor amplitude in the basal ganglia (Helmich *et al.*, 2011). Therefore, we used the GPi and GPe regions from the Basal Ganglia Human Area Template toolbox (Prodoehl *et al.*, 2008) where we previously found activity related to changes in tremor amplitude (Helmich *et al.*, 2011). Statistics were performed at the voxel level, and we corrected for multiple comparisons within our regions of interest.

For the Dynamic Causal Modelling (DCM) analyses (see below) we used inclusion masks to define the region of interest to extract the time series. We included the same five regions of interest as described above, and added the subthalamic nucleus (STN) as a hidden node (Mnearreiros *et al.*, 2013; Kahan *et al.*, 2014). The choice for these six regions was motivated by strong *a priori* evidence from previous work (Helmich *et al.*, 2011; Dirkx *et al.*, 2016). First, all of these regions show consistent tremor-related activity (Table 2) (Helmich *et al.*, 2011). Second, their inclusion allows us to model the three major pathways connecting motor cortex and basal ganglia (direct pathway, indirect pathway, hyperdirect pathway) (Redgrave *et al.*, 2010). We included the STN as a hidden node because the human STN has an estimated volume of ±240 mm^3 (Hardman *et al.*, 2002), which amounts to six voxels in native space. This leads to major partial volume effects and an unreliable BOLD time series.

BOLD functional MRI time series were extracted from five regions of interest (excluding the STN) by calculating the first eigenvariate of all voxels in the region of interest.

Localization of tremor-related activity within the ventrolateral thalamus

We tested whether the thalamic activity we report can be localized to the VIM. The VIM is analogous to the posterior ventrolateral thalamus (VLp), using the thalamic nomenclature according to Jones (Percheron *et al.*, 1996). The VLp consists of a dorsal (VLpd) and ventral (VLpv) part. In Parkinson's disease, tremor cells are mainly located in the VLpv (Magnin *et al.*, 2000). In contrast, the anterior ventrolateral thalamus (VLa) receives pallidal input.

First, we used the Morel atlas, which is based on a post-mortem examination of nine human thalami (Morel *et al.*, 1997) and has been brought in MNI space (Niemann *et al.*, 2000). We calculated the overlap between the thalamus cluster used for our DCM analyses [based on Helmich *et al.* (2011)] and thalamic nuclei derived from this atlas (Table 3). Next we statistically compared tremor amplitude-related activity (average beta value) between thalamic nuclei and sessions, using a 2 × 2 ANOVA with factors Region (VLpv versus VLa) and Dopamine (OFF versus ON) in SPSS. To gain optimal spatial resolution, we performed these analyses on data that were smoothed with a 4 mm kernel.

Second, we performed a functional connectivity analysis to verify that the VLa and VLpv (derived from the Morel atlas) are indeed functionally connected to the GPi and the cerebellum. To this end, we performed a multiple regression analysis in all 40 Parkinson's disease patients that were measured in this study (OFF session only). Our first level model included the time courses of the VLa and the VLpv (band-pass filtered between 0.008 and 0.1 Hz) and the same nuisance regressors described for our other analyses. We tested for differential thalamic connectivity (VLa versus VLpv) with the GPi and the cerebellum (see 'Regions of interest' section).

Third, we used DCM analysis to show that the optimal location of the thalamic region of interest within the tremor-related network was located between the cerebellum and motor cortex. We statistically compared two different models where our thalamic 'VIM' nucleus had either a 'VLa-like' configuration or a 'VLpv-like' configuration (Fig. 5D). We tested these two models across 15 subjects (OFF session).

Fourth, we tested whether the observed tremor-related thalamic activity was localized in a region that is anatomically connected to the cerebellum and the motor cortex. As we did not have tractography data available for our patients, we compared our functional MRI findings to a recently published study that localized the VIM using DTI tractography (Sammartino *et al.*, 2016). Thus, we compared the Euclidean distance between thalamic activity in our cohort (Table 2) and the tractographically defined VIM in MNI space (see also Helmich *et al.*, 2011).

Table 2 Tremor amplitude-related brain activity per session

Contrast	MNI (*x y z*)	T	*P*-value (FWE corr.)	MNI (*x y z*)	T	*P*-value (FWE corr.)	MNI (*x y z*)	T	*P*-value (FWE corr.)
	EMG amplitude MC (contralateral)			**VIM (contralateral)**			**Cerebellum (ipsilateral)**		
OFF	±28 −26 50	4.96	**0.014**	±12 −18 2	4.12	**0.019**	±18 −56 −20	4.19	**0.018**
ON	±36 −20 48	6.10	**0.003**	±16 −20 4	4.02	**0.024**	±12 −56 −20	4.60	**0.011**
OFF > ON	±26 −24 50	1.26	0.86	±12 −18 2	3.96	**0.025**	±14 −48 −16	1.99	0.36
	EMG change GPi (contralateral)			**GPe (contralateral)**					
OFF	±20 −4 −6	2.92	***0.091***	±22 −4 −6	3.08	0.16			
ON	±12 0 2	1.21	0.60	±18 8 0	1.99	0.59			
OFF > ON	±20 −4 −6	3.02	***0.087***	±22 −2 −6	3.94	**0.048**			

Table showing the statistical values of the tremor amplitude and changes in tremor amplitude (first temporal derivative of tremor amplitude) related activity. All values are at the voxel level and *P*-values are FWE-corrected for multiple comparisons within each region of interest. Brackets behind every region of interest indicate if it concerned the contralateral or ipsilateral side of the brain with respect to the tremor. Significant values are expressed in bold; trend significant values in bold plus italics. MC = motor cortex.

Table 3 Overlap of the tremor-related thalamus cluster with the thalamic nuclei according to the Morel atlas

Thalamic nucleus according to the Morel atlas in MNI space (Niemann *et al.*, 2000)	Overlap with thalamus region of interest used in DCM (Helmich *et al.*, 2011)
Ventral lateral posterior nucleus (VLp)	45.5%
Dorsal division (VLpd)	19.0%
Ventral division (VLpv)	28.1%
Ventral posterior medial nucleus (VPM)	10.7%
Central lateral nucleus (CL)	10.7%
Ventral posterior lateral nucleus (VPL)	14.2%
Anterior division (VPLa)	4.1%
Posterior division (VPLp)	9.0%
Ventral lateral anterior nucleus (VLa)	4.3%
Centre median nucleus (CM)	4.1%
Lateral dorsal nucleus (LD)	4.1%
Ventral medial nucleus (VM)	3.3%
Mediodorsal nucleus, parvocellular division (MDpc)	2.5%
Anteroventral nucleus (AV)	1.7%
Anterior pulvinar (PuA)	0.8%

The overlap of the thalamic cluster used for the DCM analyses [based on Helmich *et al.* (2011)] with the cytoarchitectonically defined thalamic nuclei according to the Morel atlas in MNI space (Niemann *et al.*, 2000).

Dynamic causal modelling

Defining model space

To test for the effects of dopamine on the tremor network in terms of effective connectivity we used DCM, which has been indicated as a valid method for studying cerebral effects of dopaminergic treatment in patients with Parkinson's disease (Rowe *et al.*, 2010) and has also been used to investigate effective connectivity regarding essential tremor (Buijink *et al.*, 2015; Gallea *et al.*, 2015). DCM is a Bayesian method of inference where one defines models based on predefined hypotheses to model the causal influence that one neuronal system exerts over another (Friston *et al.*, 2003). These models of interacting brain regions are built by specifying connectivity parameters between included regions of interest, including (i) fixed connections between nodes; (ii) modulation of these fixed connections by exogenous inputs; and (iii) exogenous inputs that directly cause perturbations of included nodes. These parameters are used to estimate the neural activity in each node, while haemodynamic parameters are used to translate this into a BOLD response using the haemodynamic state equation. Subsequently, these parameters are estimated into a forward model such that the predicted BOLD response provides an accurate but parsimonious explanation for observed responses—as scored by variational free energy or model evidence. The model evidence is therefore simply the probability of observing the data y under a particular model m. This model evidence can then be used for Bayesian Model Selection (BMS), a method for determining the most likely among a set of competing hypotheses (Penny *et al.*, 2004).

Here, we use a DCM model representing the cerebral tremor network based on a recently published study (Dirkx *et al.*, 2016). As in our previous study, we used stochastic DCM (Dirkx *et al.*, 2016). This is particularly important, given evidence that dopamine affects steady state stochastic BOLD dynamics within the basal ganglia (Piray *et al.*, 2016). In our previous study we investigated how the basal ganglia interact with the cerebello-thalamo-cortical circuit (variation of the endogenous connections, i.e. matrix A), and through which of the network nodes tremor is initiated (variation of the EMG-change as input, i.e. matrix C). We found consistent evidence across two independent cohorts of Parkinson's disease patients that cerebral activity associated with changes in tremor amplitude drove network activity through the GPi, and that the basal ganglia effectively influenced the cerebello-thalamo-cortical circuit through the motor cortex (but not the cerebellum). Here we continue with this winning model to determine the effects of dopamine onto this circuit by varying the modulation of dopamine onto endogenous connections (matrix B). As in our previous study, we used two-state DCM to specify inhibitory and excitatory connections between regions (Mnearreiros *et al.*, 2013; Kahan *et al.*, 2014).

To model the effects of dopamine, we first concatenated the region of interest time series over sessions (Kahan *et al.*, 2014). Subsequently, dopaminergic state was included in the models as a modulator of one of the 12 possible interregional

connections, or one of the five possible self-connections of the regions of interest. In DCM, the self-connections reflect the regional self-inhibition (Dirkx *et al.*, 2016). This is incorporated to ensure decay of activity in the absence of input and avoid exponential divergence from steady state (Friston *et al.*, 2003), which may be thought of as epileptic activity. We did not include a model where the STN self-connection was modulated by dopamine, as this was a hidden node. A hidden node could be any brain region with the connectivity fingerprint specified by the model, which means that detected effects may not be representative of the actual STN. Thus, our model space consisted of 17 models where dopamine state modulated each of the endogenous connections in turn, and an additional model with no modulation by dopamine (Fig. 2).

Bayesian model selection and parameter inference

Models were inverted using generalized filtering (Li *et al.*, 2011), which provided an estimate of the coupling parameters and model evidence. Next, we performed a random effects (RFX) BMS over our model space, thereby computing the exceedance probability and protected exceedance probability over competing models. In contrast to the exceedance probability the protected exceedance probability is more conservative as it is protected against the probability that the alternative hypothesis (i.e. model frequencies are not equal) is not true (Rigoux *et al.*, 2014).

Following inference at the model level, we proceeded to examine the parameter estimates of the winning model. Specifically, we were interested in the link between the clinical dopamine response to tremor (assessed using the UPDRS) and the response of dopamine on cerebral connectivity (estimated by DCM). Therefore, we correlated clinical tremor dopamine responsiveness (sum of UPDRS item 20 OFF minus ON) with the DCM.B parameter of the winning model (modulation of the connection by dopamine). To test whether this effect was specific for tremor we performed a partial correlation between the clinical dopamine responsiveness of tremor and the DCM.B parameter, while controlling for the clinical dopamine responsiveness of both bradykinesia (sum of UPDRS items 23–25 OFF minus ON) and rigidity (sum of UPDRS item 21 OFF minus ON). Because clinical dopamine response is a patient-bound trait and not limb-specific, we exploited all available variance and calculated brain-behaviour relationships using the total UPDRS subscores for resting tremor, bradykinesia and rigidity. To verify this assumption, we repeated these analyses for the affected upper limb only (using Spearman's rho), where we found the same results.

Results

Clinical effects of dopaminergic medication

Dopaminergic medication significantly reduced motor symptoms: the total UPDRS motor score was reduced by 24% [SD = 13%; $t(14) = 6.03$; $P < 0.001$]. Furthermore, symptom-specific analyses showed that limb bradykinesia improved by 28% [SD = 16%; $t(14) = 4.00$; $P < 0.001$], limb rigidity by 21% [SD = 12%; $t(14) = 2.47$; $P = 0.027$] and total resting tremor by 28% [SD = 40%; $t(14) = 3.30$; $P = 0.005$].

Before proceeding to the cerebral effects, we tested for possible sources of bias in our sample. First, it is unlikely that our inclusion criteria lead to a biased sample of relatively dopamine-resistant patients: the clinical dopamine response was similar between patients included in this study ($n = 15$) and the rest of the sample ($n = 25$), both for the total UPDRS [$t(38) = 0.31$; $P = 0.75$] and for resting tremor [UPDRS item 20; $t(38) = -0.21$; $P = 0.84$]. Second, it is also unlikely that the clinical dopamine response of tremor was driven by peripheral factors (e.g. gastro-intestinal malabsorption): patients with a relatively dopamine-responsive tremor (UPDRS item 20, most affected arm, OFF minus ON ≥ 1; $n = 8$) and patients with a relatively dopamine-resistant tremor (UPDRS item 20, most affected arm, OFF minus ON < 1; $n = 7$) had a similar clinical dopamine response for limb bradykinesia [$t(13) = 0.074$; $P = 0.94$] and rigidity [$t(13) = -1.17$; $P = 0.26$].

Tremor-related brain activity and effects of dopamine

We used combined EMG and functional MRI to determine the influence of dopaminergic medication on (i) tremor amplitude-related activity; and (ii) changes in tremor amplitude-related activity. Group results are shown in Fig. 1 and corresponding statistics can be found in Table 2. Using the predefined regions of interest, we found significant tremor amplitude-related activity in the cerebello-thalamo-cortical loop both in the OFF state, the ON state, and averaged across sessions. Second, we found a trend towards tremor change-related activity in the GPi only in the OFF session. Third, dopaminergic medication significantly reduced amplitude-related activity in the VIM, and it reduced change-related activity in the GPe. A whole-brain analysis revealed no additional brain areas showing an effect of dopamine on tremor-related activity.

Dynamic causal modelling

Our model comparison showed clear evidence in favour of a cerebral model in which dopamine modulated the self-connection of the VIM (model 14), indicated by a protected exceedance probability of $>99\%$ (exceedance probability of 97%; Fig. 3A). Put simply, this means that this model is >99 times more likely than any of the other models, including a null-model where no modulatory effect by dopamine was specified.

We proceeded to investigate the estimated parameters of this winning model. The modulation by dopamine of the VIM$>$VIM self-connection as estimated by DCM (i.e. Ep.B parameter) is a scaling parameter of the fixed connection strength (i.e. Ep.A parameter) where a value >1 indicates an increase of the inhibitory self-connection strength (Zeidman, 2015). A one-sample *t*-test showed that this scaling parameter was not significantly different from 1 across the whole group [$t(14)$; mean = 1.002, SD = 0.013,

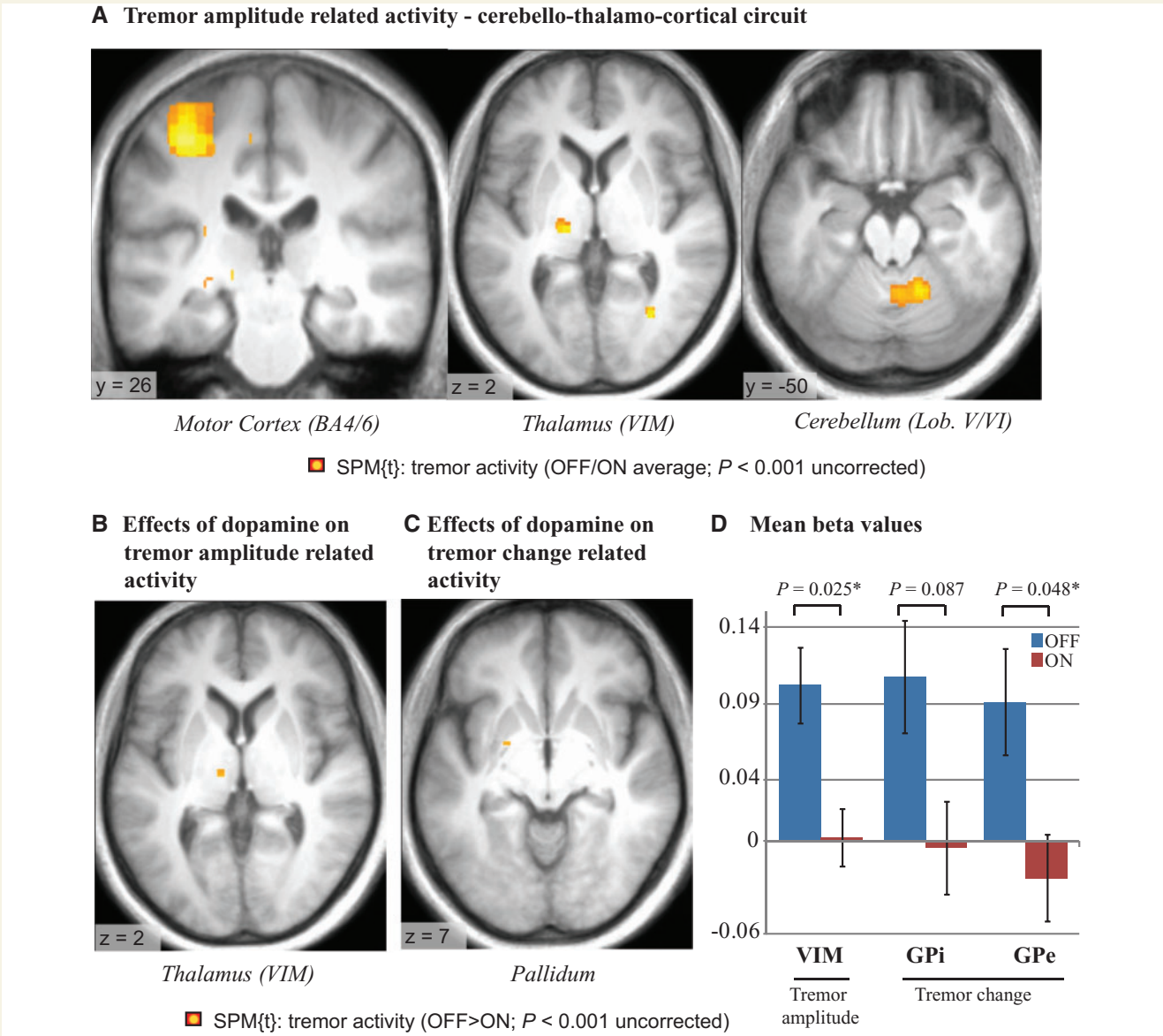

Figure 1 Tremor amplitude-related activity and effects of dopamine on this activity. All images of patients with a left-sided affected arm were flipped, so that the lateralization of the involved brain regions was the same among all subjects (i.e. corresponding to the most affected hand). (**A**) Tremor amplitude-related activity in the cerebello-thalamo-cortical circuit (OFF/ON average). (**B**) Effects of dopamine depletion (OFF > ON) on tremor amplitude-related activity. (**C**) Effects of dopamine depletion (OFF > ON) on activity related to changes in tremor amplitude; and (**D**) mean beta-values of the voxels where we found dopamine-related effects. For graphical purposes, we used a statistical threshold of $P < 0.001$ uncorrected. Statistical details are summarized in Table 2. *Significant effect.

$P = 0.48$], indicating no significant modulatory effect of dopamine on the self-connection. This is perhaps at first surprising, because this model clearly outperformed a null-model with no modulatory effect of dopamine. However, this finding emphasizes the power of Bayesian model comparison: the combination of the absence of a significant directional effect at the parameter level across the group in context of positive model evidence indicates that this parameter is highly variable across individuals, yet meaningful. Indeed, we observed a significant relationship between the dopaminergic modulation of the inhibitory VIM self-connection (Ep.B) and the clinical dopamine response of resting tremor (R = 0.56, $P = 0.03$; Fig. 4A). This indicates that dopamine increased the inhibitory VIM self-coupling most in patients with clinically more dopamine-responsive tremor.

Next, we tested whether this brain-behaviour relationship was specific for tremor. There were no correlations between the dopaminergic modulation of the inhibitory VIM self-connection (Ep.B) and the clinical dopamine response of bradykinesia (R = 0.06, $P = 0.83$; Fig. 4B) or rigidity

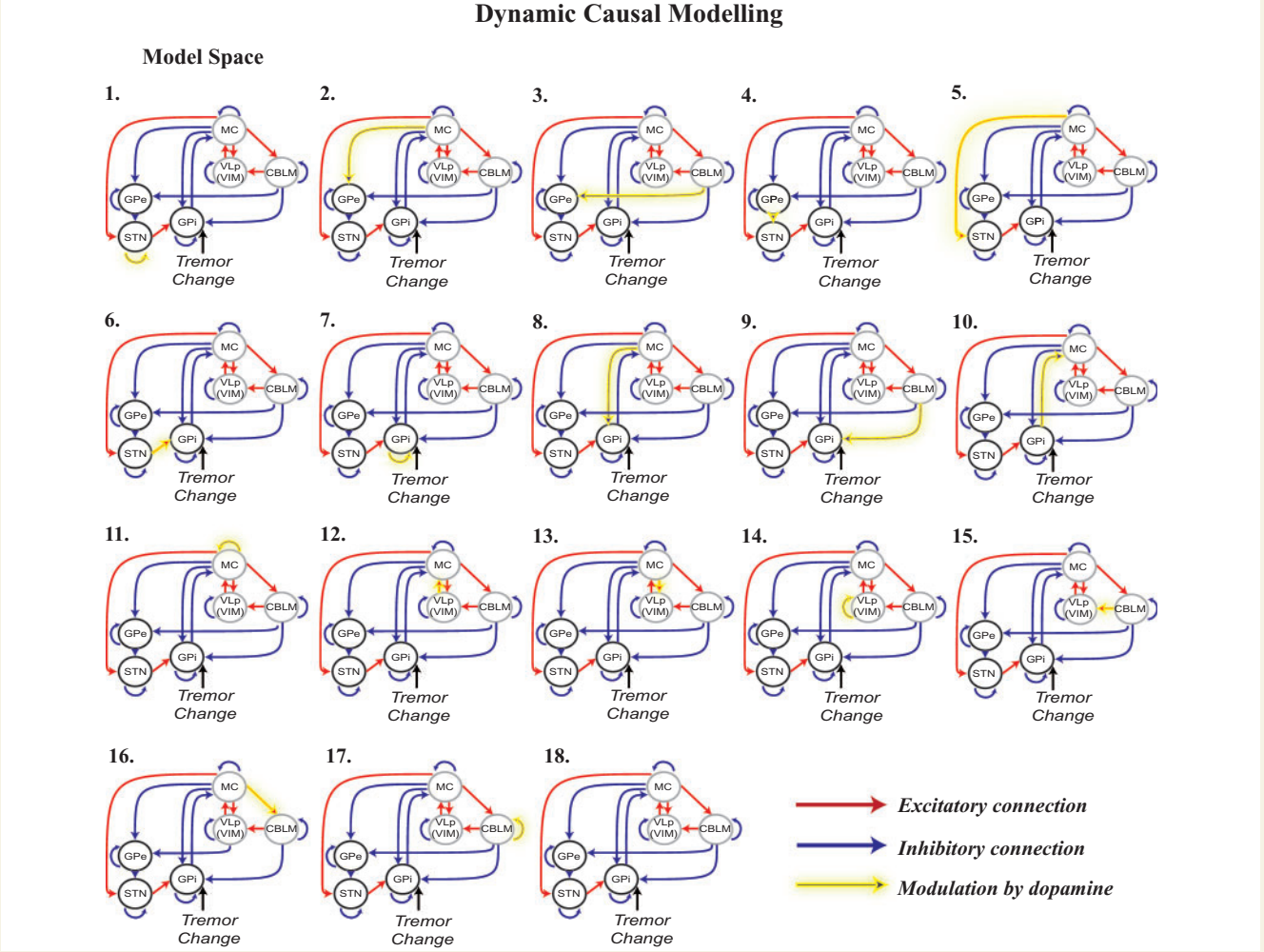

Figure 2 DCM model space. Figure shows 17 models where one of the connections was modulated by dopamine and one model (model 18) where there was no modulatory effect of dopamine.

(R = 0.42, $P = 0.11$; Fig. 4C). Furthermore, when we calculated partial correlations between each clinical symptom and dopaminergic modulation of the inhibitory VIM self-connection (Ep.B)—while controlling for the other two symptoms—we found a significant partial correlation only for resting tremor (R = 0.56, $P = 0.046$), but not for bradykinesia or rigidity.

Localization of tremor-related effects within the ventrolateral thalamus

We used several analyses to test whether the tremor-related effects we observed in the thalamus were localized in the cerebellum receiving nucleus (VLpv) or in the pallidal receiving nucleus (VLa).

First, we found that the thalamic cluster used in our DCM analyses overlapped 46% with the VLp: 28% with the VLpv and 19% with the VLpd. In contrast, only 4% of the cluster overlapped with the VLa (Fig. 5A and Table 3). The rest of the cluster overlapped with other thalamic nuclei or was not labelled (Table 3). This clearly shows that the thalamic cluster overlapped more with cerebellar than with pallidal receiving thalamic nuclei. Moreover, the effects of dopamine on tremor-related activity were specific for the VLpv [Region × Dopamine interaction: $F(1,14) = 18.3$, $P = 0.001$]. *Post hoc* comparisons showed that OFF dopamine, there was only significant tremor-related activity in the VLpv [$t(14) = 2.0$, $P = 0.036$ one-tailed], but not in the VLa [$P = 0.33$; VLpv versus VLa: $t(14) = 2.9$, $P = 0.006$ one-tailed; Fig. 5B]. Taken together, this analysis statistically localizes tremor-related activity to the cerebellar receiving thalamic nucleus (VLpv), and it localizes dopaminergic influences onto tremor-related activity in the VLpv.

Second, functional connectivity analyses showed significantly larger functional connectivity of the VLa than the VLpv with the GPi [MNI coordinates (−18 −6 2), T = 5.72, $P < 0.001$ FWE corrected for multiple comparisons across the region of interest]. Conversely, we observed

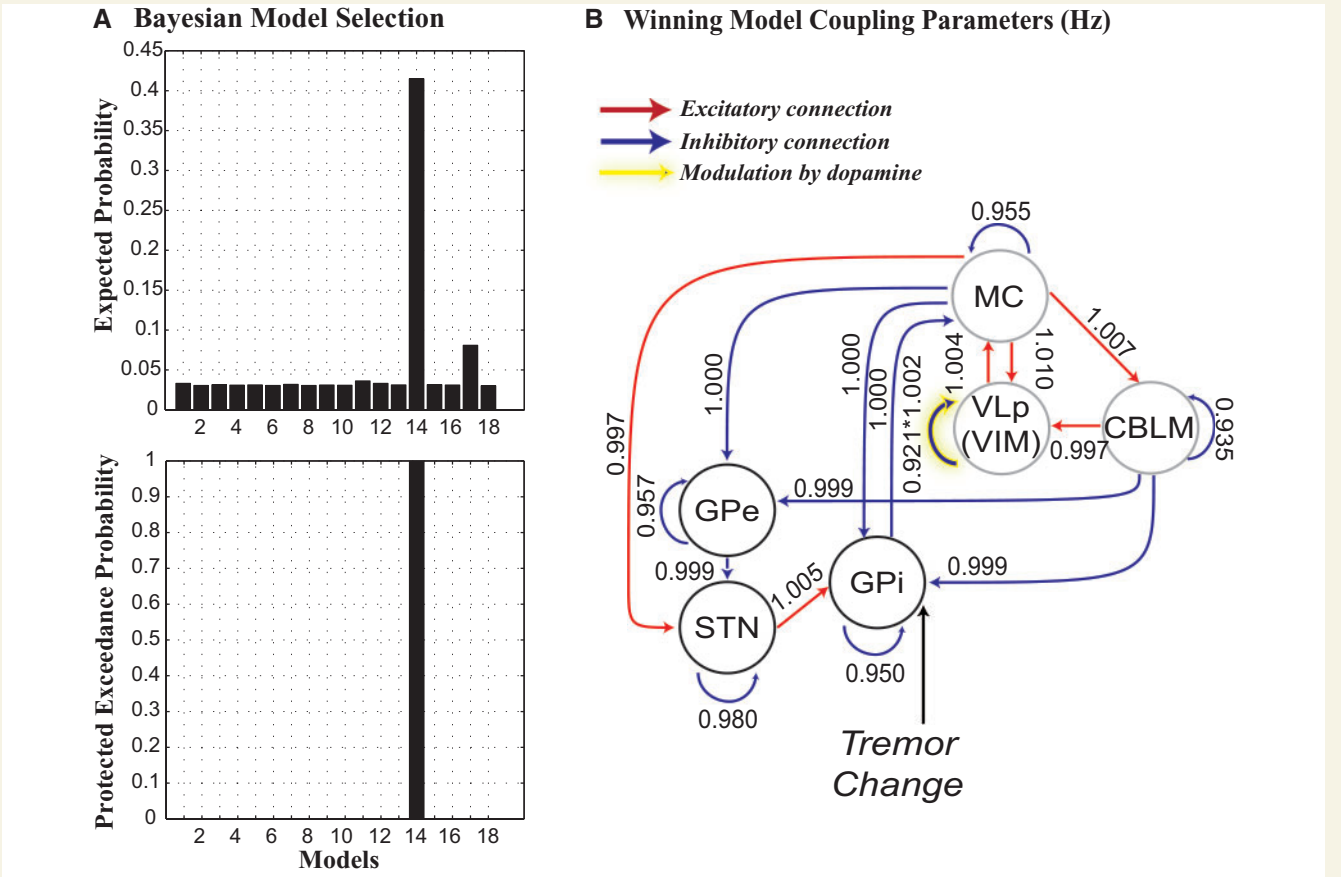

Figure 3 Results of DCM. (**A**) Bayesian Model Selection of all our models showing that model 14 is clearly the strongest. (**B**) Illustration and coupling parameters of our winning model (model 14). The net coupling parameter of the VIM > VIM self-connection is determined by the intrinsic coupling times modulation by dopamine (Ep.A × Ep.B = 0.921 × 1.002). MC = motor cortex.

significantly larger functional connectivity of the VLpv than the VLa with the cerebellum [MNI coordinates (12 −54 −14), T = 3.68, $P = 0.016$ FWE corrected; Fig. 5C]. These findings clearly show that the VLpv was functionally connected to the same cerebellar region where we observed tremor-related activity.

Third, an RFX BMS showed clear evidence in favour of a model where our thalamic 'VIM' nucleus had a 'VLpv-like configuration' as compared to a model where the VIM had a 'VLa-like configuration' (exceedance probability = 98%; protected exceedance probability = 84%; Fig. 5D). This indicates that the tremor-related activity we observed in the thalamus is localized to the cerebellar receiving region of the thalamus.

Fourth, the anatomical location of thalamic activity in our study (Table 2) closely matched the anatomical location of the VIM as identified using DTI tractography [MNI coordinates (±13.6 −17.3 −1.0) for healthy subjects; (±15.2 −18.7 −1.1) for patients with essential tremor] (Sammartino *et al.*, 2016). Specifically, the Euclidean distance between our functionally-defined VIM and the tractographically-defined VIM was 3.5 mm for healthy subjects and 4.5 mm for patients with essential tremor. This suggests that the thalamic region where we observed tremor-related activity has anatomical connections to the cerebellum (dentate) and motor cortex. In contrast, the peak voxel of the VIM (Table 2) was >10 mm away from the optimal stereotactic position for STN-DBS [±10.5 −16.7 −8.6] (Vanegas-Arroyave *et al.*, 2016). Therefore, it is unlikely that the thalamic activity reported here relates to STN.

Relationship between univariate and dynamic causal modelling results

We investigated the effects of dopamine on tremor-related cerebral activity using both univariate (BOLD response correlated with tremor signal) and multivariate (DCM) analyses.

Importantly, both analyses are consistent in that they point towards the VIM as a key target of dopaminergic medication, even though both analyses are fundamentally different. More specifically, the univariate analysis reports the effect of dopamine on the statistical dependency among tremor amplitude (EMG) and cerebral activity (functional

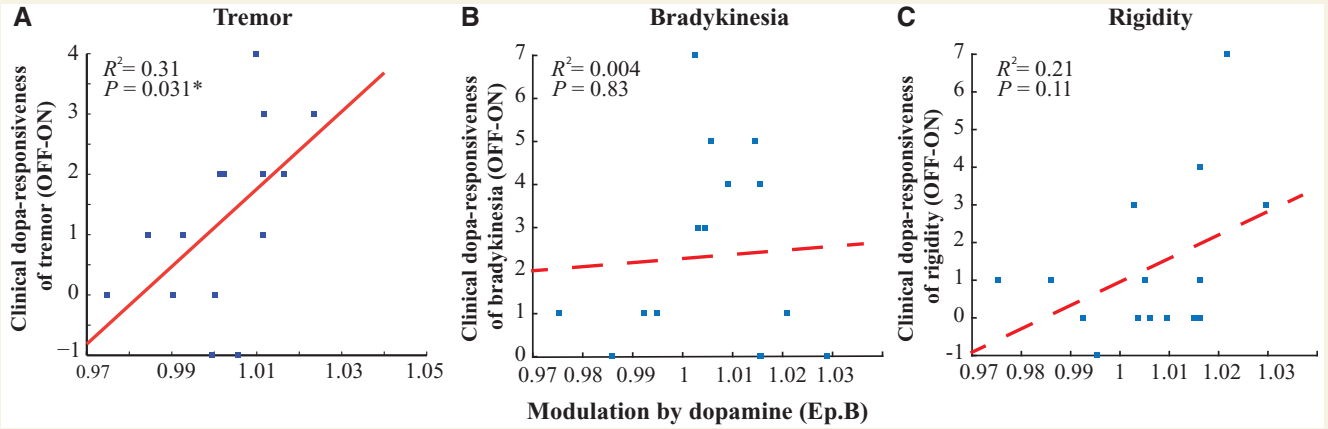

Figure 4 Brain–behaviour relationship. Figure displaying the correlation between the dopaminergic modulation of the inhibitory VIM self-connection (Ep.B) as estimated by DCM and the clinical dopamine responsiveness of resting tremor (**A**), bradykinesia (**B**), and rigidity (**C**) based on UPDRS differences score (OFF minus ON). Only dopamine responsiveness of tremor was significantly correlated with the Ep.B parameter, even when controlling for the dopamine responsiveness of the other two symptoms (partial correlation, R = 0.56, *P* = 0.046). *Significant effect.

MRI BOLD). This type of analysis does not take inter-regional dependencies into account. Thus, dopamine may influence one brain area (e.g. the basal ganglia) that in turn produces downstream effects in another brain region (e.g. the VIM). To test whether the effect of dopamine on the VIM was mediated by other nodes in the tremor circuitry, we used DCM. DCM is a multivariate approach that takes into account the tremor-related and spontaneous (stochastic) dynamics of the entire network. Therefore, statistical evidence for a particular model is not dependent on significant effects of dopamine in individual nodes (i.e. the univariate effects, Fig. 1). We compared multiple models in which we varied the site where dopamine was allowed to affect network activity. The model in which dopamine directly influenced the VIM won convincingly from other models in which dopamine influenced the basal ganglia (>99 times likely). This suggests that dopaminergic medication influenced the VIM directly, instead of indirectly through the basal ganglia.

Discussion

We investigated the cerebral mechanisms underlying the effects of dopamine on tremor. The findings show that dopaminergic medication reduced tremor amplitude-related activity in the thalamic VIM nucleus. Using DCM, we further specified the cerebral mechanisms underlying this effect: dopaminergic medication influenced VIM activity by potentiating thalamic self-inhibition, rather than acting indirectly through the basal ganglia. Furthermore, the magnitude of thalamic self-inhibition by dopamine predicted the clinical dopamine responsiveness of resting tremor. This relationship was specific for resting tremor: it was absent for the other two cardinal Parkinson's disease symptoms, bradykinesia and rigidity. Finally, we found that dopaminergic medication reduced cerebral activity related to tremor changes in the pallidum. This further specifies our previous findings that tremulous activity starts in the pallidum (Dirkx *et al.*, 2016) and that dopamine depletion in the pallidum is associated with tremor severity (Helmich *et al.*, 2011). Taken together, we show that dopamine controls Parkinson's resting tremor by acting both on the pallidum and on the cerebellar thalamus.

Dopamine modulates Parkinson's tremor through the VIM and pallidum

The VIM plays a causal role in the generation of Parkinson's tremor, as shown by the ability of VIM deep brain stimulation to reduce tremor (Lyons *et al.*, 2001; Atkinson *et al.*, 2002). Furthermore, cerebral activity in the entire cerebello-thalamo-cortical-circuit is reduced after VIM-DBS, as shown by FDG-PET (Fukuda *et al.*, 2004). Accordingly, based on functional MRI data, we have previously suggested that the VIM is involved in modulating resting tremor amplitude, analogous to a light dimmer (Helmich *et al.*, 2012). The current results show that dopamine reduces tremor-related activity in the VIM, possibly by increasing thalamic self-inhibition. In turn, this may disrupt tremor amplification by the VIM, resulting in tremor suppression. This finding fits with previous observations that levodopa specifically reduced thalamo-cortical oscillatory coupling in tremor-dominant Parkinson's disease patients (Pollok *et al.*, 2009), and that it increased the participation of the thalamus to a sensorimotor network in drug-naïve Parkinson's disease patients (Esposito *et al.*, 2013).

At a first glance, an effect of dopamine onto a cerebellar nucleus of the thalamus seems counter-intuitive, as dopamine is the major neurotransmitter of the basal ganglia (Garnett *et al.*, 1983). However, there is also evidence for direct dopaminergic projections from the midbrain to the

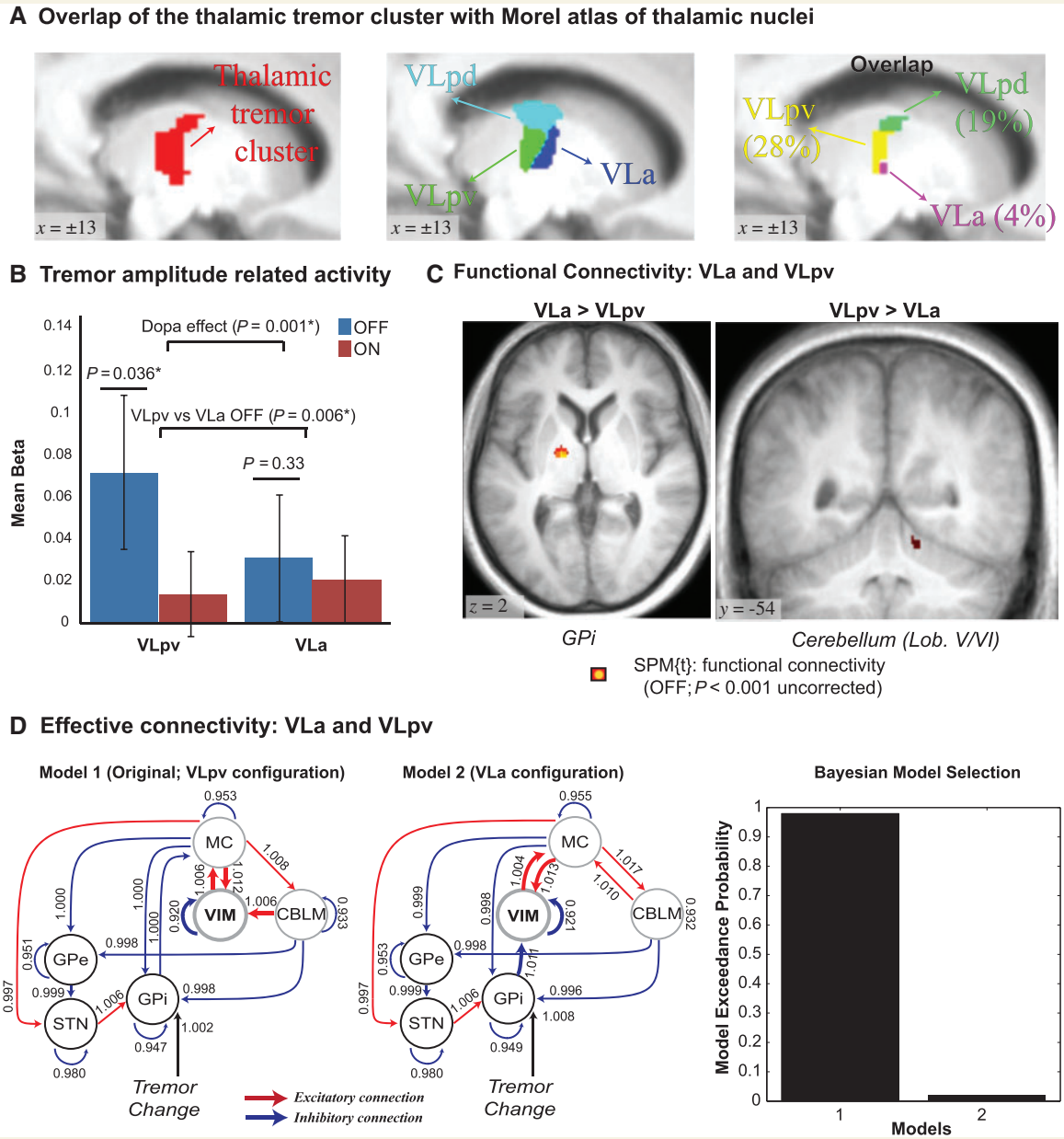

Figure 5 Localization of tremor-related activity within the ventrolateral thalamus. This figure displays the anatomical localization of the thalamic tremor-related effects reported here. (**A**) The thalamic region of interest (used in our DCM analyses, and based on Helmich *et al.*, 2011) mainly overlaps with the VLpv, but not with the VLa. (**B**) The influence of dopamine on tremor amplitude-related cerebral responses within the VLpv was significantly higher than in the VLa (averaged betas across each region). (C) The VLa shows significantly stronger functionally connectivity with the ipsilateral GPi, as compared to the VLpv. Instead, the VLpv had significantly stronger functional connectivity with the contralateral cerebellum, as compared to the VLa. (**D**) A DCM model comparison showing that a model where our thalamic cluster had a 'VLp-like' effective connectivity profile was more likely than a model where our thalamic cluster had a 'VLa-like' effective connectivity profile.

ventrolateral thalamus, including the cerebellar nuclei. For example, fluorescence spectroscopy has shown the presence of dopamine molecules in the primate thalamus (Brown *et al.*, 1979) and retrograde tracer studies in primates have demonstrated widespread dopaminergic projections to the entire thalamus, including the ventrolateral nuclei (Sanchez-Gonzalez *et al.*, 2005). Moreover, post-mortem studies in humans have shown that several thalamic nuclei exhibit DAT immunoreactive axons, including the VIM (Sanchez-Gonzalez *et al.*, 2005). In fact, DAT density in the human ventrolateral thalamus was similar to that in the primary motor cortex (Sanchez-Gonzalez *et al.*, 2005), the cortical area with the most dense dopaminergic innervations (Lewis *et al.*, 2001). In the healthy state, dopaminergic projections to the cerebello-thalamo-cortical circuit may have an important functional role: to encode the

value of forward models, enabling efficient motor learning (Schweighofer *et al.*, 2004). In primate models of Parkinson's disease, these dopaminergic projections to the motor cortex (Gaspar *et al.*, 1991) and thalamus (Freeman *et al.*, 2001) are degenerated.

In addition to the VIM, the pallidum is also one of the key players in the generation of tremor (Prodoehl *et al.*, 2013), e.g. GPi-DBS is very effective in reducing tremor (Kumar *et al.*, 2000). Accordingly, we previously showed that the GPi drives tremulous activity in a cerebello-thalamo-cortical motor loop (using functional MRI), and that pallidal (but not striatal) dopamine depletion was correlated with resting tremor severity (Helmich *et al.*, 2011; Dirkx *et al.*, 2016). The current finding that dopamine reduced tremor-related activity in the pallidum provides further support for the idea that pallidal dopamine depletion leads to tremor-related activity.

Interestingly, the mesencephalic retrorubral area, which is specifically degenerated in tremor-dominant Parkinson's disease patients (as compared to non-tremulous Parkinson's disease patients) (Hirsch *et al.*, 1992), sends dopaminergic projections to both the ventrolateral thalamus and pallidum (Jan *et al.*, 2000; Sanchez-Gonzalez *et al.*, 2005). This suggests that degeneration of dopaminergic projections from the retrorubral area may cause thalamic and pallidal dopamine depletion, and that this could be a critical factor in the development of Parkinson's resting tremor.

Impaired thalamic self-inhibition in patients with a dopamine-resistant tremor

The connectivity results suggest that dopamine increases thalamic inhibition, predicting dopamine-responsiveness of the tremor. There is conflicting evidence as to whether tremor-related activity in the thalamus is caused by an increase or decrease of inhibition. It has been suggested that the hyperpolarized cells in the thalamus might act as a tremor pacemaker. This idea is based on *in vitro* studies showing that the intrinsic biophysical properties of thalamic neurons allow them to serve as relay cells or as single cell oscillators. Specifically, slightly depolarized thalamic cells tend to oscillate at 10 Hz, while hyperpolarized cells oscillate at 6 Hz (Jahnsen and Llinas, 1984). However, the presence of this 6 Hz oscillatory mode, which is associated with low threshold calcium spike bursts, has been questioned in patients with Parkinson's disease (Zirh *et al.*, 1998).

The finding that successful tremor suppression was associated with increased thalamic self-inhibition contradicts the idea that increased thalamic inhibition causes Parkinson's tremor. In contrast, dopamine-dependent thalamic self-inhibition may be a physiological mechanism that protects the thalamus from a permanent oscillatory state. This mechanism could be represented by the thalamic reticulate nucleus or local circuit neurons, which both use GABA to inhibit the VIM (Kultas-Ilinsky *et al.*, 2003) and are sensitive to dopamine (Sanchez-Gonzalez *et al.*, 2005). More specifically, the reticulate nucleus has been proposed to be an important modulator of thalamo-cortical communication (Lam and Sherman, 2011), and has been recently hypothesized to play a role in Parkinson's tremor (Duval *et al.*, 2015). The idea that dopamine suppresses tremor by potentiating thalamic inhibition suggests that it works similar to VIM deep brain stimulation, which has been suggested to reduce tremor by inducing local inhibitory mechanisms (Dostrovsky and Lozano, 2002).

Dopamine only increased thalamic inhibition in patients with a relatively dopamine-responsive tremor. This suggests that there may be non-dopaminergic brain regions contributing to dopamine-resistant tremor. One possibility is that the degeneration of other neurotransmitter systems, such as the noradrenergic (Isaias *et al.*, 2011) or serotonergic (Doder *et al.*, 2003) systems, may have more significant contributions to dopamine-resistant tremor than the dopamine system. This is supported by the fact that the reticulate nucleus is modulated not only by the dopaminergic system, but also by the noradrenergic and serotonergic systems (Pratt and Morris, 2015). The fact that VIM-DBS is an effective treatment in both dopamine-resistant and dopamine-responsive patients (Lozano *et al.*, 2002) suggests that it is able to increase thalamic self-inhibition independent of the underlying neurotransmitter abnormality. Future studies might focus on alternative (pharmacological) therapies targeting thalamic inhibition in dopamine-resistant patients.

Interpretational issues

We included the STN as a hidden node in the network, given our limited spatial resolution. In this way, we incorporated the influence of STN onto the network given its location within the circuit, without using the own region's measured BOLD signal (Kahan *et al.*, 2014). We verified that addition of the STN as a hidden node did not critically influence our results, by repeating the analyses without the STN (i.e. by directly connecting the GPi to the GPe via an inhibitory connection). This gave the same results: the model where dopamine influenced the VIM was significantly stronger than all others (protected exceedance probability of $>98\%$).

Head motion may be a major confound when comparing functional MRI data across sessions. However, head motion did not significantly differ between sessions, subjects did not abruptly move their heads during scanning, and we regressed out motion artefacts by including a global signal (Power *et al.*, 2014) and an extensive set of movement parameters into our analysis (Lund *et al.*, 2005). Thus, we are confident that our results are not biased by motion artefacts.

The nature of our study prevented us from using a group of healthy subjects as control group. However, our main aim was to test for the interaction between dopamine and tremor-related activity, and this interaction cannot be tested in subjects without tremor (i.e. healthy controls). A

previous study has shown that tremor-related activity in Parkinson's disease patients is different from activity related to mimicked tremor in healthy subjects (Muthuraman *et al.*, 2012). This difference may relate to the fact that resting tremor in Parkinson's disease is involuntary, whereas mimicked tremor is voluntary per definition. Furthermore, investigating what the influence of dopamine is on a voluntary-related tremor network in healthy, non-dopamine depleted subjects seems even more problematic.

The results of a DCM analysis depend explicitly upon the models evaluated. Here we contrasted different models where dopamine modulates a single node or a single effective connection. Thus, we tested where in the circuit dopamine has the largest effect, rather than exploring all possible modulations within our model.

Conclusion

The findings suggest that dopamine controls Parkinson's tremor by acting on the cerebellar thalamus (VIM) and on the pallidum. We propose that dopamine suppresses resting tremor by potentiating thalamic inhibition, thereby preventing tremor amplification in this region. This contradicts the hypothesis that tremor is caused by thalamic hyperpolarization, i.e. increased inhibition. We propose that patients with a relatively dopamine-resistant tremor have impaired dopaminergic control over the thalamus, possibly due to changes in other neurotransmitter systems.

Funding

M.D. and R.H. were funded by a grant of the Dutch Brain Foundation (grant F2013(1)-15 to R.H.). H.d.O. was supported by a Research Veni Grant from the Innovational Research Incentives Scheme of the Netherlands Organisation for Scientific Research.

Supplementary material

Supplementary material is available at *Brain* online.

References

Atkinson JD, Collins DL, Bertrand G, Peters TM, Pike GB, Sadikot AF. Optimal location of thalamotomy lesions for tremor associated with Parkinson disease: a probabilistic analysis based on postoperative magnetic resonance imaging and an integrated digital atlas. J Neurosurg 2002; 96: 854–66.

Berger B, Gaspar P, Verney C. Dopaminergic innervation of the cerebral cortex: unexpected differences between rodents and primates. Trends Neurosci 1991; 14: 21–7.

Brown RM, Crane AM, Goldman PS. Regional distribution of monoamines in the cerebral cortex and subcortical structures of the rhesus monkey: concentrations and *in vivo* synthesis rates. Brain Res 1979; 168: 133–50.

Buijink AW, van der Stouwe AM, Broersma M, Sharifi S, Groot PF, Speelman JD, et al. Motor network disruption in essential tremor: a functional and effective connectivity study. Brain 2015; 138 (Pt 10): 2934–47.

Dirkx MF, den Ouden H, Aarts E, Timmer M, Bloem BR, Toni I, et al. The cerebral network of Parkinson's tremor: an effective connectivity fMRI study. J Neurosci 2016; 36: 5362–72.

Doder M, Rabiner EA, Turjanski N, Lees AJ, Brooks DJ; 11C-WAY 100635 PET study. Tremor in Parkinson's disease and serotonergic dysfunction: an 11C-WAY 100635 PET study. Neurology 2003; 60: 601–15.

Dostrovsky JO, Lozano AM. Mechanisms of deep brain stimulation. Mov Disord 2002; 17 (Suppl 3): S63–8.

Duval C, Daneault JF, Hutchison WD, Sadikot AF. A brain network model explaining tremor in Parkinson's disease. Neurobiol Dis 2015; 85: 49–59.

Esposito F, Tessitore A, Giordano A, De Micco R, Paccone A, Conforti R, et al. Rhythm-specific modulation of the sensorimotor network in drug-naive patients with Parkinson's disease by levodopa. Brain 2013; 136 (Pt 3): 710–25.

Fishman PS. Paradoxical aspects of parkinsonian tremor. Mov Disord 2008; 23: 168–73.

Freeman A, Ciliax B, Bakay R, Daley J, Miller RD, Keating G, et al. Nigrostriatal collaterals to thalamus degenerate in parkinsonian animal models. Ann Neurol 2001; 50: 321–9.

Friston KJ, Harrison L, Penny W. Dynamic causal modelling. Neuroimage 2003; 19: 1273–302.

Fukuda M, Barnes A, Simon ES, Holmes A, Dhawan V, Giladi N, et al. Thalamic stimulation for parkinsonian tremor: correlation between regional cerebral blood flow and physiological tremor characteristics. Neuroimage 2004; 21: 608–15.

Gallea C, Popa T, Garcia-Lorenzo D, Valabregue R, Legrand AP, Marais L, et al. Intrinsic signature of essential tremor in the cerebello-frontal network. Brain 2015; 138 (Pt 10): 2920–33.

Garcia-Cabezas MA, Martinez-Sanchez P, Sanchez-Gonzalez MA, Garzon M, Cavada C. Dopamine innervation in the thalamus: monkey versus rat. Cereb Cortex 2009; 19: 424–34.

Garnett ES, Firnau G, Nahmias C. Dopamine visualized in the basal ganglia of living man. Nature 1983; 305: 137–8.

Gaspar P, Duyckaerts C, Alvarez C, Javoy-Agid F, Berger B. Alterations of dopaminergic and noradrenergic innervations in motor cortex in Parkinson's disease. Ann Neurol 1991; 30: 365–74.

Hardman CD, Henderson JM, Finkelstein DI, Horne MK, Paxinos G, Halliday GM. Comparison of the basal ganglia in rats, marmosets, macaques, baboons, and humans: volume and neuronal number for the output, internal relay, and striatal modulating nuclei. J Comp Neurol 2002; 445: 238–55.

Helmich RC, Hallett M, Deuschl G, Toni I, Bloem BR. Cerebral causes and consequences of parkinsonian resting tremor: a tale of two circuits? Brain 2012; 135 (Pt 11): 3206–26.

Helmich RC, Janssen MJ, Oyen WJ, Bloem BR, Toni I. Pallidal dysfunction drives a cerebellothalamic circuit into Parkinson tremor. Ann Neurol 2011; 69: 269–81.

Hirsch EC, Mouatt A, Faucheux B, Bonnet AM, Javoy-Agid F, Graybiel AM, et al. Dopamine, tremor, and Parkinson's disease. Lancet 1992; 340: 125–6.

Hurley MJ, Mash DC, Jenner P. Markers for dopaminergic neurotransmission in the cerebellum in normal individuals and patients with Parkinson's disease examined by RT-PCR. Eur J Neurosci 2003; 18: 2668–72.

Isaias IU, Marzegan A, Pezzoli G, Marotta G, Canesi M, Biella GE, et al. A role for locus coeruleus in Parkinson tremor. Front Hum Neurosci 2011; 5: 179.

Jahnsen H, Llinas R. Ionic basis for the electro-responsiveness and oscillatory properties of guinea-pig thalamic neurones *in vitro*. J Physiol 1984; 349: 227–47.

Jan C, Francois C, Tande D, Yelnik J, Tremblay L, Agid Y, et al. Dopaminergic innervation of the pallidum in the normal state, in

MPTP-treated monkeys and in parkinsonian patients. Eur J Neurosci 2000; 12: 4525–35.
Kahan J, Urner M, Moran R, Flandin G, Marreiros A, Mancini L, et al. Resting state functional MRI in Parkinson's disease: the impact of deep brain stimulation on 'effective' connectivity. Brain 2014; 137 (Pt 4): 1130–44.
Kish SJ, Shannak K, Hornykiewicz O. Uneven pattern of dopamine loss in the striatum of patients with idiopathic Parkinson's disease. Pathophysiologic and clinical implications. N Engl J Med 1988; 318: 876–80.
Kultas-Ilinsky K, Sivan-Loukianova E, Ilinsky IA. Reevaluation of the primary motor cortex connections with the thalamus in primates. J Comp Neurol 2003; 457: 133–58.
Kumar R, Lang AE, Rodriguez-Oroz MC, Lozano AM, Limousin P, Pollak P, et al. Deep brain stimulation of the globus pallidus pars interna in advanced Parkinson's disease. Neurology 2000; 55 (12 Suppl 6): S34–9.
Lam YW, Sherman SM. Functional organization of the thalamic input to the thalamic reticular nucleus. J Neurosci 2011; 31: 6791–9.
Lewis DA, Melchitzky DS, Sesack SR, Whitehead RE, Auh S, Sampson A. Dopamine transporter immunoreactivity in monkey cerebral cortex: regional, laminar, and ultrastructural localization. J Comp Neurol 2001; 432: 119–36.
Li B, Daunizeau J, Stephan KE, Penny W, Hu D, Friston K. Generalised filtering and stochastic DCM for fMRI. Neuroimage 2011; 58: 442–57.
Lindvall O, Bjorklund A. The organization of the ascending catecholamine neuron systems in the rat brain as revealed by the glyoxylic acid fluorescence method. Acta Physiol Scand Suppl 1974; 412: 1–48.
Lozano AM, Dostrovsky J, Chen R, Ashby P. Deep brain stimulation for Parkinson's disease: disrupting the disruption. Lancet Neurol 2002; 1: 225–31.
Lund TE, Norgaard MD, Rostrup E, Rowe JB, Paulson OB. Motion or activity: their role in intra- and inter-subject variation in fMRI. Neuroimage 2005; 26: 960–4.
Lyons KE, Koller WC, Wilkinson SB, Pahwa R. Long term safety and efficacy of unilateral deep brain stimulation of the thalamus for parkinsonian tremor. J Neurol Neurosurg Psychiatry 2001; 71: 682–4.
Magnin M, Morel A, Jeanmonod D. Single-unit analysis of the pallidum, thalamus and subthalamic nucleus in parkinsonian patients. Neuroscience 2000; 96: 549–64.
Mnearreiros AC, Cagnan H, Moran RJ, Friston KJ, Brown P. Basal ganglia-cortical interactions in Parkinsonian patients. Neuroimage 2013; 66: 301–10.
Morel A, Magnin M, Jeanmonod D. Multiarchitectonic and stereotactic atlas of the human thalamus. J Comp Neurol 1997; 387: 588–630.
Mounayar S, Boulet S, Tande D, Jan C, Pessiglione M, Hirsch EC, et al. A new model to study compensatory mechanisms in MPTP-treated monkeys exhibiting recovery. Brain 2007; 130 (Pt 11): 2898–914.
Muthuraman M, Heute U, Arning K, Anwar AR, Elble R, Deuschl G, et al. Oscillating central motor networks in pathological tremors and voluntary movements. What makes the difference? Neuroimage 2012; 60: 1331–9.
Niemann K, Mennicken VR, Jeanmonod D, Morel A. The Morel stereotactic atlas of the human thalamus: atlas-to-MR registration of internally consistent canonical model. Neuroimage 2000; 12: 601–16.
Oostenveld R, Fries P, Maris E, Schoffelen JM. FieldTrip: Open source software for advanced analysis of MEG, EEG, and invasive electrophysiological data. Comput Intell Neurosci 2011; 2011: 156869.
Penny WD, Stephan KE, Mechelli A, Friston KJ. Modelling functional integration: a comparison of structural equation and dynamic causal models. Neuroimage 2004; 23 (Suppl 1): S264–74.
Percheron G, Francois C, Talbi B, Yelnik J, Fenelon G. The primate motor thalamus. Brain Res Brain Res Rev 1996; 22: 93–181.
Piray P, den Ouden HE, van der Schaaf ME, Toni I, Cools R. Dopaminergic modulation of the functional ventrodorsal architecture of the human striatum. Cereb Cortex 2016, in press.
Pirker W. Correlation of dopamine transporter imaging with parkinsonian motor handicap: how close is it? Mov Disord 2003; 18 (Suppl 7): S43–51.
Pogarell O, Gasser T, van Hilten JJ, Spieker S, Pollentier S, Meier D, et al. Pramipexole in patients with Parkinson's disease and marked drug resistant tremor: a randomised, double blind, placebo controlled multicentre study. J Neurol Neurosurg Psychiatry 2002; 72: 713–20.
Pollok B, Makhloufi H, Butz M, Gross J, Timmermann L, Wojtecki L, et al. Levodopa affects functional brain networks in Parkinsonian resting tremor. Mov Disord 2009; 24: 91–8.
Power JD, Mitra A, Laumann TO, Snyder AZ, Schlaggar BL, Petersen SE. Methods to detect, characterize, and remove motion artifact in resting state fMRI. Neuroimage 2014; 84: 320–41.
Pratt JA, Morris BJ. The thalamic reticular nucleus: a functional hub for thalamocortical network dysfunction in schizophrenia and a target for drug discovery. J Psychopharmacol 2015; 29: 127–37.
Prodoehl J, Planetta PJ, Kurani AS, Comella CL, Corcos DM, Vaillancourt DE. Differences in brain activation between tremor- and nontremor-dominant Parkinson disease. JAMA Neurol 2013; 70: 100–6.
Prodoehl J, Yu H, Little DM, Abraham I, Vaillancourt DE. Region of interest template for the human basal ganglia: comparing EPI and standardized space approaches. Neuroimage 2008; 39: 956–65.
Qamhawi Z, Towey D, Shah B, Pagano G, Seibyl J, Marek K, et al. Clinical correlates of raphe serotonergic dysfunction in early Parkinson's disease. Brain 2015; 138 (Pt 10): 2964–73.
Redgrave P, Rodriguez M, Smith Y, Rodriguez-Oroz MC, Lehericy S, Bergman H, et al. Goal-directed and habitual control in the basal ganglia: implications for Parkinson's disease. Nat Rev Neurosci 2010; 11: 760–72.
Rigoux L, Stephan KE, Friston KJ, Daunizeau J. Bayesian model selection for group studies—revisited. Neuroimage 2014; 84: 971–85.
Rowe JB, Hughes LE, Barker RA, Owen AM. Dynamic causal modelling of effective connectivity from fMRI: are results reproducible and sensitive to Parkinson's disease and its treatment? Neuroimage 2010; 52: 1015–26.
Sammartino F, Krishna V, King NK, Lozano AM, Schwartz ML, Huang Y, et al. Tractography-based ventral intermediate nucleus targeting: novel methodology and intraoperative validation. Mov Disord 2016; 31: 1217–25.
Sanchez-Gonzalez MA, Garcia-Cabezas MA, Rico B, Cavada C. The primate thalamus is a key target for brain dopamine. J Neurosci 2005; 25: 6076–83.
Schweighofer N, Doya K, Kuroda S. Cerebellar aminergic neuromodulation: towards a functional understanding. Brain Res Brain Res Rev 2004; 44: 103–16.
Timmermann L, Gross J, Dirks M, Volkmann J, Freund HJ, Schnitzler A. The cerebral oscillatory network of parkinsonian resting tremor. Brain 2003; 126 (Pt 1): 199–212.
Vanegas-Arroyave N, Lauro PM, Huang L, Hallett M, Horovitz SG, Zaghloul KA, et al. Tractography patterns of subthalamic nucleus deep brain stimulation. Brain 2016; 139 (Pt 4): 1200–10.
Zeidman P. SPM/Two State DCM. 2015. https://en.wikibooks.org/wiki/SPM/Two_State_DCM (11 March 2015, date last accessed).
Zirh TA, Lenz FA, Reich SG, Dougherty PM. Patterns of bursting occurring in thalamic cells during parkinsonian tremor. Neuroscience 1998; 83: 107–21.